



LAWRENCE  
LIVERMORE  
NATIONAL  
LABORATORY

# Calibration of the Lawrence Livermore National Laboratory Passive-Active Neutron Drum Shuffler for Measurement of Highly Enriched Uranium in Oxides within DOE-STD-3013-2000 Containers

M. E. Mount, W. J. O'Connell

June 9, 2005

Institute of Nuclear Materials Management, 46th Annual Meeting  
Phoenix, AZ, United States  
July 10, 2005 through July 14, 2005

## **Disclaimer**

---

This document was prepared as an account of work sponsored by an agency of the United States Government. Neither the United States Government nor the University of California nor any of their employees, makes any warranty, express or implied, or assumes any legal liability or responsibility for the accuracy, completeness, or usefulness of any information, apparatus, product, or process disclosed, or represents that its use would not infringe privately owned rights. Reference herein to any specific commercial product, process, or service by trade name, trademark, manufacturer, or otherwise, does not necessarily constitute or imply its endorsement, recommendation, or favoring by the United States Government or the University of California. The views and opinions of authors expressed herein do not necessarily state or reflect those of the United States Government or the University of California, and shall not be used for advertising or product endorsement purposes.

# **Calibration of the Lawrence Livermore National Laboratory Passive-Active Neutron Drum Shuffler for Measurement of Highly Enriched Uranium in Oxides within DOE-STD-3013-2000 Containers**

Mark Mount, Lawrence Livermore National Laboratory  
7000 East Avenue, L-347, Livermore, CA 94550, USA (925) 422-9800  
William O'Connell, Lawrence Livermore National Laboratory  
7000 East Avenue, L-195, Livermore, CA 94550, USA (925) 422-8789

## **Abstract**

Lawrence Livermore National Laboratory (LLNL) uses the LLNL passive-active neutron drum (PAN) shuffler (Canberra Model JCC-92) for accountability measurement of highly enriched uranium (HEU) oxide and HEU in mixed uranium-plutonium (U-Pu) oxide. In June 2002, at the 43<sup>rd</sup> Annual Meeting of the Institute of Nuclear Material Management, LLNL reported on an extensive effort to calibrate this shuffler, based on standards measurements and extensive simulations, for HEU oxides and mixed U-Pu oxides in thin-walled primary and secondary containers. In August 2002, LLNL began to also use DOE-STD-3013-2000 containers for HEU oxide and mixed U-Pu oxide. These DOE-STD-3013-2000 containers are comprised of a stainless steel convenience can enclosed in welded stainless steel primary and secondary containers. Compared to the double thin-walled containers, the DOE-STD-3013-2000 containers have substantially thicker walls, and the density of materials in these containers was found to extend over a greater range (1.35 g/cm<sup>3</sup> to 4.62 g/cm<sup>3</sup>) than foreseen for the double thin-walled containers. Further, the DOE-STD-3013-2000 Standard allows for oxides containing at least 30 wt% Pu plus U whereas the calibration algorithms for thin-walled containers were derived for virtually pure HEU or mixed U-Pu oxides. An initial series of Monte Carlo simulations of the PAN shuffler response to given quantities of HEU oxide and mixed U-Pu oxide in DOE-STD-3013-2000 containers was generated and compared with the response predicted by the calibration algorithms for thin-walled containers. Results showed a decrease on the order of 10% in the count rate, and hence a decrease in the calculated U mass for measured unknowns, with some varying trends versus U mass. Therefore a decision was made to develop a calibration algorithm for the PAN shuffler unique to the DOE-STD-3013-2000 container. This paper describes that effort and selected unknown item measurement results.

## **Introduction**

In June 2002, at the 43<sup>rd</sup> Annual Meeting of the Institute of Nuclear Material Management, Lawrence Livermore National Laboratory (LLNL) reported on an extensive effort to calibrate the LLNL passive-active neutron drum (PAN) shuffler (Canberra Model JCC-92) for accountability measurements of highly enriched uranium (HEU) oxides and HEU in mixed uranium-plutonium (U-Pu) oxides in thin-walled primary and secondary containers [1, 2] with nominal wall thickness of 0.2 mm and 0.3 mm, respectively. The calibration algorithms were based on standards and working reference materials (WRMs) measurements and an extensive series of Monte Carlo simulations of the PAN shuffler response to the standards and WRMs, including variations in the material density (2.4 g/cm<sup>3</sup> to 4.8 g/cm<sup>3</sup>), container diameter (5.24 cm to 12.17 cm inside diameter), and <sup>235</sup>U enrichment (20.107 wt% to 93.1959 wt%). Figure 1 below shows details typical of the simulation models used to represent the double thin-walled containers.

---

This work was performed under the auspices of the U.S. Department of Energy by the University of California, Lawrence Livermore National Laboratory under Contract No. W-7405-Eng-48.

In August 2002, LLNL began an effort to consolidate selected HEU oxide and HEU in mixed U-Pu oxide holdings through confinement in DOE-STD-3013-2000 containers that consist of a stainless steel convenience can enclosed in welded stainless steel primary and secondary containers with nominal wall thickness of 1.0, 1.5, and 3.0 mm, respectively. Since the inside diameter of the DOE-STD-3013-2000 convenience can (11.00 cm) was within the inner thin-walled container diameter range, the expectation was that the calibration algorithms for thin-walled containers would suffice for the DOE-STD-3013-2000 containers. However, this was not to be the case as differences between measured and book values were much larger than one would predict for previously measured materials. When subsequent estimates of the density of materials in the DOE-STD-3013-2000 containers based on radiographic images were found to extend over a greater range ( $1.35 \text{ g/cm}^3$  to  $4.62 \text{ g/cm}^3$ ) than that foreseen for the double thin-walled containers, a series of Monte Carlo simulations of the PAN shuffler response to given quantities of HEU oxide and mixed U-Pu oxide in DOE-STD-3013-2000 containers was generated and compared with the response predicted by the calibration algorithms for thin-walled containers. Figure 1 below shows details typical of the simulation models used to represent the DOE-STD-3013-2000 containers. Results showed a decrease on the order of 10% in the count rate, and hence a decrease in the calculated U mass for measured unknowns. Upon consideration of the simulation results and the fact that the DOE-STD-3013-2000 Standard [3] allows for oxides containing at least 30 wt% Pu plus U, whereas the calibration algorithms for thin-walled containers were derived for virtually pure HEU or mixed U-Pu oxides, a decision was made to develop a calibration algorithm for the PAN shuffler unique to the DOE-STD-3013-2000 container.

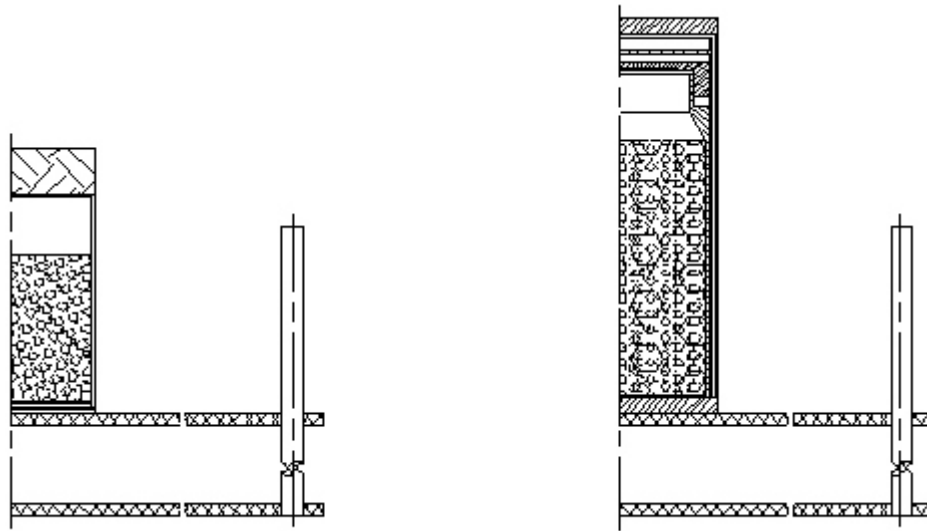


Figure 1. Left illustration is typical of the simulation models for the double thin-walled containers showing the primary container, packaging materials, secondary container, and cut-away of the sample stand. Right illustration is typical of the simulation models for the DOE-STD-3013-2000 containers showing the convenience can, primary container, secondary container, and cut-away of the sample stand.

### Calibration Plan

Because no standards or WRMs could be sacrificed to permanent confinement within DOE-STD-3013-2000 containers, the calibration is based exclusively on Monte Carlo simulations of the PAN shuffler response. The simulations were performed with the MCNP code [4] using the technique and post-processor developed by Rinard [5]. Components of the calibration plan include (1) Monte Carlo simulations of the PAN shuffler response sensitivity to variations in  $\text{U}_3\text{O}_8$  density,  $\text{PuO}_2$  density, and mixed U-Pu oxide density and relative

composition; (2) Monte Carlo simulations of the PAN shuffler response sensitivity to variations in composition and concentration of impurities in  $\text{U}_3\text{O}_8$ -bearing materials,  $\text{PuO}_2$ -bearing materials, and mixed U-Pu oxide-bearing materials; and (3) the development of a set of  $\text{U}_3\text{O}_8$ ,  $\text{PuO}_2$ , and mixed U-Pu oxide calibration algorithms and their associated errors.

*Monte Carlo Simulations of PAN Shuffler Response Sensitivity to Variations in  $\text{U}_3\text{O}_8$  Density,  $\text{PuO}_2$  Density, and Mixed U-Pu Oxide Density and Relative Composition*

Response sensitivities to variations in  $\text{U}_3\text{O}_8$  density were evaluated for seven different densities (1.2 g/cm<sup>3</sup>, 1.8 g/cm<sup>3</sup>, 2.4 g/cm<sup>3</sup>, 3.0 g/cm<sup>3</sup>, 3.6 g/cm<sup>3</sup>, 4.2 g/cm<sup>3</sup>, and 4.8 g/cm<sup>3</sup>) using  $\text{U}_3\text{O}_8$  of an elemental and isotopic composition (93.1959 wt% <sup>235</sup>U) equal to that of the LLNL unit of certified reference material (CRM) 149 [1] and mass range that varied in irregular increments from a minimum of 50 g to a nominal maximum (2230.79 g to 5576.96 g) that was a function of a fixed fill height for the convenience can and density under evaluation.

Response sensitivities to variations in  $\text{PuO}_2$  density were evaluated for the seven different densities (1.2 g/cm<sup>3</sup>, 1.8 g/cm<sup>3</sup>, 2.4 g/cm<sup>3</sup>, 3.0 g/cm<sup>3</sup>, 3.6 g/cm<sup>3</sup>, 4.2 g/cm<sup>3</sup>, and 4.8 g/cm<sup>3</sup>) using  $\text{PuO}_2$  of an elemental and isotopic composition (94.2295 wt% <sup>239</sup>Pu) equal to the average of the LLNL PuOSQ WRMs [2] and mass range that varied in irregular increments from a minimum of 50 g to a nominal maximum identical to that used for the  $\text{U}_3\text{O}_8$  density simulations (2230.79 g to 5576.96 g) .

Response sensitivities to variations in mixed U-Pu oxide density and relative composition of  $\text{U}_3\text{O}_8$  and  $\text{PuO}_2$  were evaluated for mixtures of the above referenced  $\text{U}_3\text{O}_8$  and the above referenced  $\text{PuO}_2$ . The evaluation proceeded in three steps. In the first step, responses to a mixture of 50 wt%  $\text{U}_3\text{O}_8$ - and 50 wt%  $\text{PuO}_2$ -bearing materials were simulated for the same broad range of total masses and densities as were done for the  $\text{U}_3\text{O}_8$  and  $\text{PuO}_2$  above. In the second step, responses to mixtures ranging from 10 wt%  $\text{U}_3\text{O}_8$ - and 90 wt%  $\text{PuO}_2$ -bearing materials to 90 wt%  $\text{U}_3\text{O}_8$ - and 10 wt%  $\text{PuO}_2$ -bearing materials in increments of 10 wt% were simulated for mass ranges within 1883.94 g to 5651.81 g, where the upper limit was constrained by the mixed U-Pu oxide density and the convenience can fill volume. In the third step, responses to a mixture of 50 wt%  $\text{U}_3\text{O}_8$ - and 50 wt%  $\text{PuO}_2$ -bearing materials were simulated over a mass and density range with lower mixed U-Pu oxide densities, representing mixed U-Pu oxide mixed with an inert impurity. A detailed discussion of impurities may be found in the following section. Treatment of different isotopic compositions of  $\text{U}_3\text{O}_8$  and  $\text{PuO}_2$  may be found in the section detailing development of the calibration algorithm.

*Monte Carlo Simulations of PAN Shuffler Response Sensitivity to Variations in the Composition and Concentration of Impurities in  $\text{U}_3\text{O}_8$ -bearing Materials,  $\text{PuO}_2$ -bearing Materials, and Mixed U-Pu Oxide-bearing Materials*

With allowance for oxides containing at least 30 wt% Pu plus U, a significant fraction of the DOE-STD-3013-2000 container contents may consist of impurities. Precisely what the impurities and their concentrations are in each DOE-STD-3013-2000 container is not known, nevertheless, estimates of their effect on the PAN shuffler response may still be made. Expert estimates of possible impurities in LLNL DOE-STD-3013-2000 container materials include  $\text{H}_2\text{O}$ ,  $\text{BeO}$ ,  $\text{NaOH}$ ,  $\text{NaCl}$ ,  $\text{MgO}$ ,  $\text{MgCl}_2$ ,  $\text{Al}_2\text{O}_3$ ,  $\text{CaO}$ ,  $\text{CaCl}_2$ ,  $\text{Cr}_2\text{O}_3$ ,  $\text{Fe}_2\text{O}_3$ ,  $\text{NiO}$ ,  $\text{FeCr}_2\text{O}_4$ ,  $\text{NiFe}_2\text{O}_4$ , and  $\text{Ta}_2\text{O}_5$  [6].

Response sensitivities to variations in composition and concentration of impurities in  $\text{U}_3\text{O}_8$ -bearing materials were evaluated in three steps. In the first step, response sensitivities to variations in composition and concentration of impurities in  $\text{U}_3\text{O}_8$ -bearing materials were evaluated for seven different densities (1.2 g/cm<sup>3</sup>, 1.8 g/cm<sup>3</sup>, 2.4 g/cm<sup>3</sup>, 3.0 g/cm<sup>3</sup>, 3.6 g/cm<sup>3</sup>, 4.2 g/cm<sup>3</sup>, and 4.8 g/cm<sup>3</sup>) using incrementally varying mixtures of the above referenced  $\text{U}_3\text{O}_8$  and the above possible impurities at a fixed total mass (1883.94 g). In the case of

H<sub>2</sub>O, a single mixture of 99.5 wt% U<sub>3</sub>O<sub>8</sub> and 0.5 wt% H<sub>2</sub>O, the DOE-STD-3013-2000 Standard limit [3] was used. For NaOH, mixtures of 10 wt% U<sub>3</sub>O<sub>8</sub> and 90 wt% NaOH, 90 wt% U<sub>3</sub>O<sub>8</sub> and 10 wt% NaOH, and 97.775 wt% U<sub>3</sub>O<sub>8</sub> and 2.225 wt% NaOH were used, the latter providing a hydrogen weight percent equivalent to that in 0.5 wt% H<sub>2</sub>O. In the case of BeO, NaCl, MgO, MgCl<sub>2</sub>, Al<sub>2</sub>O<sub>3</sub>, CaO, and CaCl<sub>2</sub>, mixtures of 10 wt% U<sub>3</sub>O<sub>8</sub> and 90 wt% impurity, 30 wt% U<sub>3</sub>O<sub>8</sub> and 70 wt% impurity, 50 wt% U<sub>3</sub>O<sub>8</sub> and 50 wt% impurity, 70 wt% U<sub>3</sub>O<sub>8</sub> and 30 wt% impurity, and 90 wt% U<sub>3</sub>O<sub>8</sub> and 10 wt% impurity were used. For Cr<sub>2</sub>O<sub>3</sub>, Fe<sub>2</sub>O<sub>3</sub>, NiO, FeCr<sub>2</sub>O<sub>4</sub>, NiFe<sub>2</sub>O<sub>4</sub>, and Ta<sub>2</sub>O<sub>5</sub>, mixtures of 10 wt% U<sub>3</sub>O<sub>8</sub> and 90 wt% impurity and 90 wt% U<sub>3</sub>O<sub>8</sub> and 10 wt% impurity were used. In the second step, responses were simulated for pure U<sub>3</sub>O<sub>8</sub> using the same U<sub>3</sub>O<sub>8</sub> masses and packing volumes within the container as with the impurities evaluated, but with no impurities. Then the U<sub>3</sub>O<sub>8</sub> density and geometry are the same as in the cases with impurities, but the overall density is lower. In the third step, response sensitivities from step one were compared to the appropriate response sensitivities from step two to provide an indication of the relative change in count rate derived from the presence of a given impurity.

For the NaCl, MgCl<sub>2</sub>, CaCl<sub>2</sub>, and Ta<sub>2</sub>O<sub>5</sub> impurities, their presence was found to reduce the count rate on the order of 20% or less compared to the same U<sub>3</sub>O<sub>8</sub> mass extending over the same packing volume but with no impurity. For the H<sub>2</sub>O, MgO, Al<sub>2</sub>O<sub>3</sub>, CaO, Cr<sub>2</sub>O<sub>3</sub>, Fe<sub>2</sub>O<sub>3</sub>, NiO, FeCr<sub>2</sub>O<sub>4</sub>, and NiFe<sub>2</sub>O<sub>4</sub> impurities, their presence was found to increase the count rate on the order of no more than 6%. For the BeO and NaOH impurities, their presence was found to increase the count rate on the order of 18% to 500%, respectively.

Response sensitivities to variations in composition and concentration of impurities in PuO<sub>2</sub>-bearing materials were evaluated in a similar way. A subset of the impurities was evaluated compared to the evaluations with U<sub>3</sub>O<sub>8</sub>. Specifically, the CaCl<sub>2</sub> and Ta<sub>2</sub>O<sub>5</sub> impurities which reduced the count rate with U<sub>3</sub>O<sub>8</sub>, the H<sub>2</sub>O impurity which caused a slight increase in the count rate with U<sub>3</sub>O<sub>8</sub>, and the BeO and NaOH impurities which increased the count rate with U<sub>3</sub>O<sub>8</sub> were selected. The resulting changes in count rate with PuO<sub>2</sub> were similar in direction but not as pronounced as with U<sub>3</sub>O<sub>8</sub>.

Response sensitivities to variations in composition and concentration of impurities in mixed U-Pu oxide-bearing materials were evaluated in the same way as for PuO<sub>2</sub>-bearing materials but by using a mixture of 50 wt% U<sub>3</sub>O<sub>8</sub>- and 50 wt% PuO<sub>2</sub>-bearing materials. The resulting changes in count rates were intermediate between those for the U<sub>3</sub>O<sub>8</sub> and PuO<sub>2</sub> cases, although not a linear average of those two cases.

#### *Development of a Set of U<sub>3</sub>O<sub>8</sub>, PuO<sub>2</sub>, and Mixed U-Pu Oxide Calibration Algorithms and Their Associated Errors*

The intended use of the algorithm is to provide a correspondence between the delayed-neutron count rate and the mass of U present, given the total net mass, the fill height inside the container, the U and Pu isotopics, and the Pu mass present as determined by other measurements. The approach to the algorithm is similar to that used in our earlier simulation study of thin-walled containers [7]. Basically, the series of MCNP simulations described above is used as the basis. Curves of count rate versus U mass are developed for a series of values of the other parameters just mentioned. Based on detailed information in the MCNP simulation results, separate curves are developed for the delayed neutrons generated by each isotopic species and for the net counting efficiency for delayed neutrons. The curves are parameterized, first transforming into the delayed neutron production rate versus an effective linear density to align the curves, reducing the scale of interpolation needed between MCNP-simulated cases. The same formulation of a “representative” or “effective” linear density is used as in our earlier simulation study of thin-walled containers [7]. Figure 2 shows the MCNP-simulated curves for delayed neutron production from <sup>235</sup>U in mixed U-Pu oxide and in pure U<sub>3</sub>O<sub>8</sub>. The fraction of the <sup>239</sup>Pu linear density to be added to that of the <sup>235</sup>U is selected to be a value that provides for closely stepped curves for neighboring percentages of U<sub>3</sub>O<sub>8</sub> in the mixed U-Pu oxide.

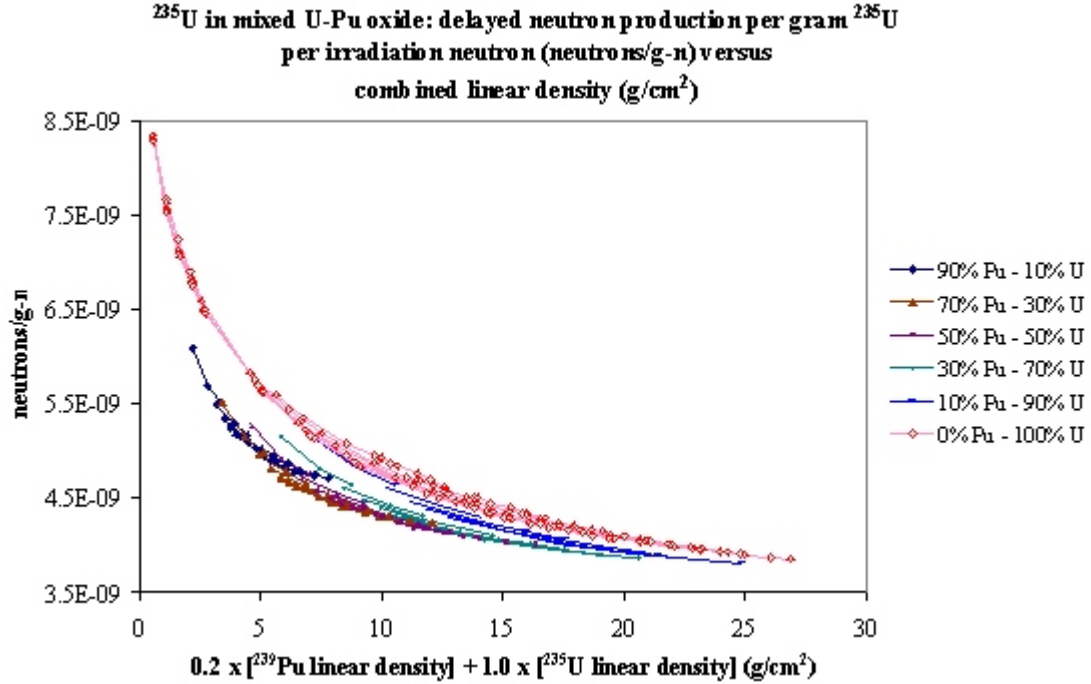


Figure 2. Delayed neutron production from  $^{235}\text{U}$ , per gram of  $^{235}\text{U}$  per irradiation neutron, versus combined linear density, for a selected series of  $\text{PuO}_2$ -and- $\text{U}_3\text{O}_8$  mixtures and pure  $\text{U}_3\text{O}_8$  in DOE-STD-3013-2000 containers over the range of oxide densities simulated.

For each MCNP-simulated curve, a functional curve is fitted using equations of differing types and a fitting procedure as described in our earlier simulation study of thin-walled containers [7]. For  $^{235}\text{U}$  in a mixed U-Pu oxide, the equation type is a sum of two declining exponentials plus a constant. For  $^{235}\text{U}$  in  $\text{U}_3\text{O}_8$ , an additional declining exponential is added to the equation, because the simulated data extend over a broader mass range as described earlier. For  $^{238}\text{U}$  in a mixed U-Pu oxide or  $\text{U}_3\text{O}_8$ , the equation type is a straight line plus a declining exponential. For the net counting efficiency, a straight line is used. Then for given conditions including assumed U mass values, the delayed neutron counting rate is evaluated using these fitted equations for the delayed neutron production rate and net counting efficiency. For intermediate values in weight percent  $\text{U}_3\text{O}_8$ , the delayed neutron production rate is evaluated by interpolation on the curve parameters, except between 90 wt%  $\text{U}_3\text{O}_8$  and 100 wt%  $\text{U}_3\text{O}_8$ , where interpolation is done on the curve values. The rate per irradiation neutron is converted to a rate per second using the  $^{252}\text{Cf}$  source strength. Finally, for a given measured count rate, the U mass is determined by an inverse solution of the equation of count rate versus U mass.

A similar procedure is used for delayed neutrons from Pu isotopes. Figure 3 shows the MCNP-simulated curves for delayed neutron production from  $^{239}\text{Pu}$  in mixed U-Pu oxide and in pure  $\text{PuO}_2$ . For  $^{239}\text{Pu}$  in a mixed U-Pu oxide, the equation type is a sum of a declining exponential plus a straight line. For  $^{239}\text{Pu}$  in  $\text{PuO}_2$ , an additional declining exponential is added to the equation, because the simulated data extend over a broader mass range. For  $^{240}\text{Pu}$  in a mixed U-Pu oxide or  $\text{PuO}_2$ , the equation type is a straight line plus a declining exponential, as for  $^{238}\text{U}$ . The count rates from  $^{241}\text{Pu}$  and  $^{241}\text{Am}$  are treated as being proportional to the count rates from  $^{239}\text{Pu}$  and  $^{240}\text{Pu}$ , respectively. This is an adequate approximation given their small contribution.

A low effective linear density of fissile isotopes could occur either because the container is filled only to a low fill height, or because the fissile material is diluted by impurities. The impurity study described above included simulations of the  $\text{U}_3\text{O}_8$  and/or  $\text{PuO}_2$  at low densities, the same as their densities would be as diluted

by impurities, but simulated without the impurities. As seen in Figure 3, the situation of low density extending over a large fill volume gives up to a 3% higher delayed neutron production rate, and is the more usual case with the filled DOE-STD-3013-2000 containers. Hence, the low-density MCNP-simulated results were used for the low linear density range of the curves to be fitted for use in the calibration algorithm.

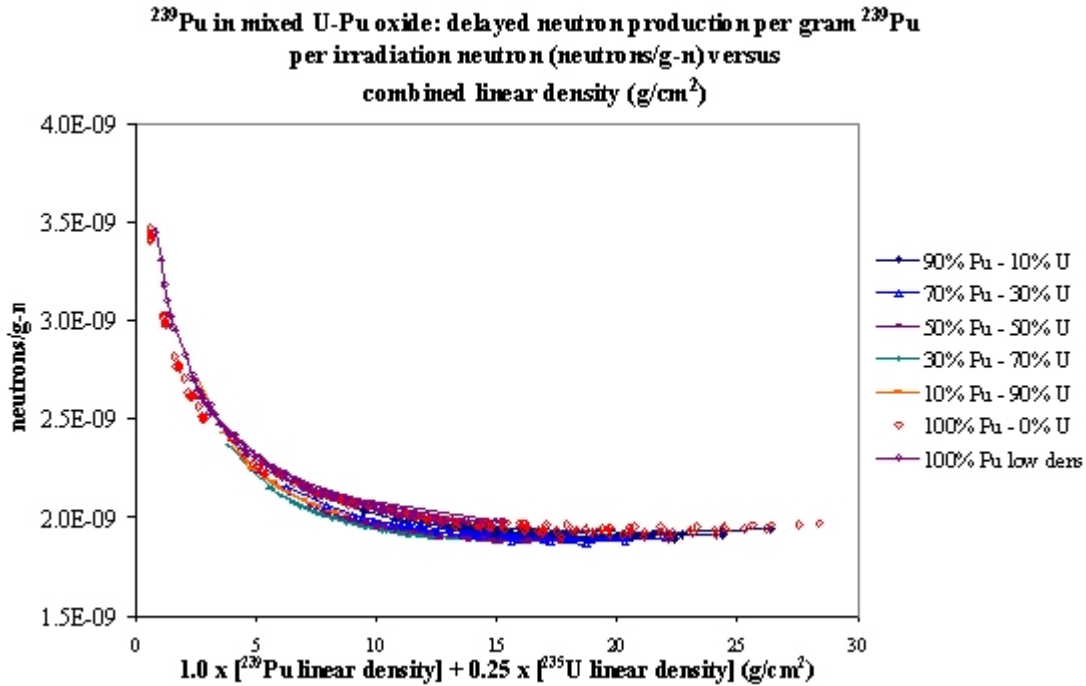


Figure 3. Delayed neutron production from  $^{239}\text{Pu}$ , per gram of  $^{239}\text{Pu}$  per irradiation neutron, versus combined linear density, for a selected series of  $\text{PuO}_2$ -and- $\text{U}_3\text{O}_8$  mixtures and pure  $\text{PuO}_2$  in DOE-STD-3013-2000 containers over the range of oxide densities simulated.

For lower isotopic percentages of either  $^{235}\text{U}$  or  $^{239}\text{Pu}$ , findings from our earlier simulation study [7] were used. It was found that the delayed neutron production rate from the fissile isotopes was dependent on the effective linear density of the fissile isotope and not separately dependent on the fissile isotopes percentage, with deviations from this principle ranging from essentially zero up to a few percent in production rate as the percent of fissile isotopes got down to 20 wt%. For fissionable isotopes such as  $^{238}\text{U}$  and  $^{240}\text{Pu}$ , their delayed neutron production rate was dependent on only the effective linear density of the fissile isotope while within the low to medium effective linear density range, and showed deviations from this when the effective linear density of the fissile isotopes was near the upper end of its feasible range and the percent of fissile isotopes was near 50 wt% or lower. In the present set of DOE-STD-3013-2000 container measurements, the ratio of fissile isotopes mass to total U plus Pu mass is always greater than 60 wt%, so a correction for the percent of fissile isotopes is not necessary.

The error in determination of U mass has several components. The measured count rate error depends on the signal rate and the background rate. The impurities can elevate or decrease the signal count rate, as discussed above. The weight percent of impurities is known approximately, but the atomic species present in a given case is generally not known. We estimate the effect due to impurities to be neutral at best estimate, with an uncertainty at one sigma of 0.25 times the weight percent impurities, e.g.,  $\pm 12.5\%$  uncertainty in count rate at 50 wt% impurities, and varying linearly with the weight percent of impurities. The Pu-based delayed neutron count rate is to be subtracted from the signal to get the U-based count rate. The modeling error in the Pu-based count rate is estimated to be 2%. The modeling error in the U-based count rate versus U mass is estimated to be 2%.



In high-enriched U,  $^{235}\text{U}$  produces most of the count rate. A low-enriched U sample is a small-signal sample. The most challenging measurements of U mass are for a small U signal, whether from small mass compared to the Pu or low enrichment, in the presence of a large Pu mass and/or large background (which depends both on the Pu and the environment of the measurement) and/or relatively large weight percent impurities. The error in U mass determination is calculated for each specific measurement case.

### Selected Unknown Item Measurement Results

Table 1 summarizes the measurement results for a selected set of LLNL unknown mixed U-Pu oxide items chosen to demonstrate the applicability of the LLNL PAN shuffler mixed U-Pu oxide calibration algorithms. These items cover extensive ranges in measured Pu mass (135.29 g to 4069.88 g), declared material density (1.72 g/cm<sup>3</sup> to 4.37 g/cm<sup>3</sup>), declared U mass (10.29 g to 4204.00 g), declared  $^{235}\text{U}$  enrichment (40.00 wt%  $^{235}\text{U}$  to 94.49 wt%  $^{235}\text{U}$ ), and declared U-Pu mass fraction (30.50 wt% U-Pu to 86.57 wt% U-Pu).

**Table 1. Summary of measurement results for selected LLNL mixed U-Pu oxide items.**

Item Identifier	Measured		Declared				Measured U mass (g)	U mass difference (g)
	Material mass (g)	Pu mass <sup>1</sup> (g)	Material density (g/cm <sup>3</sup> )	U mass (g)	$^{235}\text{U}$ fraction (wt%)	U-Pu fraction (wt%)		
MRF007395	4974.60	135.29	2.87	4204.00	93.51	86.57	4038.56 ± 81.14	165.44
MRF007396	4999.80	4069.88	4.28	32.58	69.22	82.07	111.08 ± 54.37	-78.50
MRF007397	4999.50	3468.13	3.67	24.81	63.92	69.87	36.57 ± 103.49	-11.76
MRF007398	3436.30	1533.83	1.95	24.25	93.08	45.90	73.96 ± 71.75	-49.71
MRF007399	4998.70	658.50	3.35	3664.08	94.49	86.47	3580.15 ± 72.32	83.92
MRF007425	4984.30	664.51	3.65	3613.18	94.37	85.82	3523.00 ± 71.96	90.18
MRF007426	4877.10	1010.00	3.64	2873.37	85.31	79.57	2851.03 ± 85.65	22.34
MRF007428	4969.30	1740.00	3.24	2168.18	93.91	78.55	2275.39 ± 68.35	-107.21
MRF007429	4983.50	2477.24	4.23	1709.47	88.56	84.01	1652.63 ± 52.88	56.84
MRF007458	4850.10	2612.70	3.40	1039.00	93.57	75.54	1119.70 ± 74.28	-80.70
MRF007459	3803.10	1746.12	2.48	252.79	92.38	52.56	61.92 ± 83.68	190.87
MRF007590	2714.90	1082.16	1.97	195.46	79.32	47.06	186.59 ± 76.42	8.86
MRF007591	3341.40	1072.30	1.80	110.57	83.70	35.40	110.60 ± 78.13	-0.03
MRF007593	3366.10	1262.10	2.25	88.01	94.20	40.11	34.36 ± 67.05	53.65
MRF007594	3414.50	1001.42	1.84	45.71	46.75	30.50	87.28 ± 110.66	-41.57
MRF007595	3002.60	1215.57	1.72	40.66	69.48	41.84	49.01 ± 77.33	-8.35
MRF007596	4184.00	1598.64	2.30	38.33	52.91	39.13	36.85 ± 131.60	1.48
MRF007597	2795.60	1513.35	1.92	34.80	40.00	55.38	36.58 ± 107.20	-1.78
MRF007601	4800.10	3889.64	4.37	10.99	88.56	83.35	24.18 ± 43.52	-13.19
MRF007602	2431.10	1296.25	2.37	10.29	94.16	53.75	36.67 ± 47.01	-26.38
<b>Total</b>							20180.51 ± 361.54	254.41

1. Decayed to the date of the PAN shuffler measurement.

Because of the very nature of the items themselves (i.e., unknowns with measured values for Pu mass and experimenter declared values for U mass), the spread exhibited in the individual differences between the declared and measured U mass and the total U mass difference is not unexpected. While the measured U mass results reflect the accountability values for these items and are therefore not subject to an inventory difference analysis, the total U mass difference of 254.41 g is no more than 1.26% of the total measured U mass and well within the standard deviation ( $\pm 361.54$  g) and the 95% confidence limit ( $\pm 708.61$  g) in the total measured U mass.

### Conclusion

Measurement results obtained to date clearly indicate that the PAN shuffler is a useful tool for accountability measurements of HEU when relatively large quantities of HEU are present in mixed U-Pu oxide materials. For the more challenging measurements of HEU mass where the U signal is small, whether from small mass compared to the Pu or low enrichment, in the presence of a large Pu mass and/or large background and/or relatively large weight percent impurities, the usefulness of the PAN shuffler measurements may be limited to a verification role. More measurements are currently in process to determine the threshold between accountability and verification measurements.

### References

- [1] M. E. Mount, W. J. O'Connell, C. W. Cochran, P. M. Rinard, D. M. Dearborn, and E. D. Endres, Update on the Calibration of the Lawrence Livermore National Laboratory Passive-Active Neutron Drum Shuffler for Measurement of Highly Enriched Uranium Oxide, in *Proceedings of the Institute of Nuclear Materials Management, 43<sup>rd</sup> Annual Meeting*, Orlando, FL, June 23-27, 2002.
- [2] M. E. Mount, W. J. O'Connell, C. W. Cochran, P. M. Rinard, D. M. Dearborn, and E. D. Endres, Calibration of the Lawrence Livermore National Laboratory Passive-Active Neutron Drum Shuffler for Measurement of Highly Enriched Uranium Oxide in Mixed Oxide, in *Proceedings of the Institute of Nuclear Materials Management, 43<sup>rd</sup> Annual Meeting*, Orlando, FL, June 23-27, 2002.
- [3] "Stabilization, Packaging, and Storage of Plutonium-Bearing Materials," U.S. Department of Energy, Washington, DC (2000), DOE-STD-3013-2000.
- [4] J. F. Briesmeister, Editor, *MCNP<sup>TM</sup> -- A General Monte Carlo N-Particle Transport Code, Version 4C*, LA-13709-M, Los Alamos National Laboratory, March 2000.
- [5] P. M. Rinard, "Calculating Accurate Shuffler Count Rates with Applications," in *Proceedings of the 42<sup>nd</sup> Annual Meeting, Institute of Nuclear Materials Management*, Indian Wells, CA, July 15-19, 2001.
- [6] O. Krikorian, Personal communication, Lawrence Livermore National Laboratory, Livermore, CA, September 2004.
- [7] W. J. O'Connell, C. W. Cochran, and M. E. Mount, Performance Model for the Lawrence Livermore National Laboratory Passive-Active Neutron Drum Shuffler, in *Proceedings of the Institute of Nuclear Materials Management, 44<sup>rd</sup> Annual Meeting*, Phoenix, AZ, July 13-17, 2003.